PERGAMON

International Journal of Heat and Mass Transfer 43 (2000) 1661–1672

International Journal of HEAT and MASS TRANSFER

www.elsevier.com/locate/ijhmt

Thermal radiation from nonisothermal spherical particles of a semitransparent material

Leonid A. Dombrovsky

Heat Transfer Department, Institute for High Temperatures of the Russian Academy of Sciences, Krasnokazarmennaya 17A, Moscow 111250, Russia

Abstract

The applicability of radiation transfer theory for calculations of the thermal radiation emitted by spherical particle of a semitransparent material, and in particular the determination of radial heat generation profiles, is analyzed. For homogeneous isothermal particles, a comparison with the exact solution based on the Mie theory shows that the radiation transfer calculations are sufficiently accurate for diffraction parameter of the particle of $x \geq 20$. Numerical examples for large particles illustrate the transition from conditions of dominant radiation of the central region of the particle to conditions of the surface layer emission. A new differential approximation for radiation transfer in a refracting particle is proposed. This approximation called MDP_0 (modified DP_0) is much simpler than the radiation transfer equation. Using MDP_0, we have a chance to consider radiation–conduction interaction in nonisothermal particles without great computational efforts.

Keywords: Heat; Radiation; Emission; Particle; Oxide

1. Introduction

In analyzing radiation heat transfer in disperse systems containing particles up to hundreds of microns in size, a single particle is usually considered to be isothermal. This assumption greatly simplifies the calculation of the thermal radiation of the particle. At the same time, in the case of intensive cooling, the temperature difference between the center and the surface of the particle may be considerable. One example is the problem of vapor explosion in a nuclear reactor severe accident due to thermal interaction of molten uranium oxide droplets having initial temperature of about 3200 K with ambient boiling water [1].

Thermal radiation of a nonisothermal particle is an especially interesting problem for particles of a semitransparent material (in particular, for metal oxide particles). The point is that materials, which are semitransparent in the infrared spectral range, are usually characterized by low thermal conductivity and, as a result, by a comparatively large temperature difference between the center and the surface of the particle. On the other hand, in the case of a small index of absorption, the solution to the problem is expected to be more complex because of the possible considerable contribution of radiation emitted from the central high-temperature core of the particle.

A rigorous statement of the problem must take into account effects of interference as is done in the Mie theory. At the same time, in the case of large particles, for which the temperature difference is

PII: S0017-9310(99)00231-8

Nomenclature

a	particle radius
a_k, b_k, c_k, d_k	Mie coefficients
B_λ	Planck's function
C_1, C_2	coefficients in Eq. (36)
D	dimensionless radiation diffusion coefficient
E_r, E_θ, E_ϕ	amplitudes of electric field components
E_0	electric field amplitude in the incident wave
g, h, g_0, h_0	dimensionless functions defined by Eqs. (19) and (33)
i	$i=\sqrt{-1}$
I	radiation intensity
k	thermal conductivity
l	relative ray length in Eq. (29)
m	complex index of refraction
n	index of refraction
N_a, N_m	parameters of diffusion approximation, see comments to (28)
p	local heat generation rate
P	angle-averaged heat generation rate
q	radiative flux
$\bar{q}$	relative radiative flux in Eq. (39)
q_conv	convective heat flux
Q_a	absorption efficiency factor
r	radial coordinate
$\bar{r}$	dimensionless coordinate, r/a
R, $R_{\parallel}$, $R_{\perp}$	Fresnel's reflection coefficient
S	dimensionless heat generation function defined by Eq. (7)
T	temperature
$\bar{T}$	average temperature in Eq. (25)
W	dimensionless heat generation rate defined by Eq. (15)
x	diffraction parameter
y	independent variable in Eq. (21)

Greek symbols

α_k, β_k, γ_k	mathematical functions in Eq. (3)
γ, $\gamma^{(1)}$	coefficients of boundary conditions in Eqs. (20) and (34)
ε	particle emissivity
θ	angle measured from the incident wave direction in (5) or from the radius-vector one in Eq. (9)
κ	index of absorption
λ	radiation wavelength
μ	angular coordinate, $\mu=\cos\theta$
μ_c, μ_*	values of μ defined by Eqs. (11) and (32)
π_k, τ_k	Mie angular functions in Eq. (5)
ρ	current diffraction parameter, $\rho=\bar{r}x$
Σ_a	absorption coefficient
τ, τ_0	optical thickness, see Eqs. (14) and (15)
φ	dimensionless radiation intensity
ϕ	azimuth angle
ψ_k, ζ_k	Riccati–Bessel functions

Subscripts

av	average temperature
k	order of mathematical functions
r	radial component
s	particle surface
λ	spectral dependent
θ, ϕ	angular components
e	external

more important, one can try to use the geometrical optics approximation and the radiation transfer theory. In recent papers [2–4], it was shown that geometrical optics is a reasonable approximation for the calculating the energy-density distribution inside large nonabsorbing spherical particles. It is important that the geometrical-optics results show the main features of the Mie solution and provide a physical explanation of the electromagnetic interactions inside particles, which are large in comparison with the wavelength of radiation.

The main objective of this paper is to determine the range of applicability of the radiation transfer theory for calculation of the heat generation distribution inside a particle and to develop a simple differential approximation, which would be proper for the solution to the spectral radiative–conductive problem.

2. The exact Mie solution for an isothermal particle

The thermal radiation emitted by a homogeneous isothermal spherical particle of arbitrary material may be calculated using the well-known exact Mie solution. It is sufficient to determine the value of the absorption efficiency factor Q_a, which is a function of the diffraction parameter $x=2\pi a/\lambda$ and the complex index of refraction $m = n - i\kappa$ [5–7]. The absorption efficiency factor is usually calculated as the difference between the extinction and the scattering efficiency factors. The corresponding equation is as follows [5–7]:

$$Q_a = \frac{2}{x^2}\sum_{k=1}^{\infty}(2k+1)\Big[\mathrm{Re}(a_k) - |a_k|^2 + \mathrm{Re}(b_k) - |b_k|^2\Big] \tag{1}$$

where the Mie coefficients are

$$a_k = \frac{\psi_k(x)\psi_k'(mx) - m\psi_k'(x)\psi_k(mx)}{\zeta_k(x)\psi_k'(mx) - m\zeta_k'(x)\psi_k(mx)}$$
$$b_k = \frac{m\psi_k(x)\psi_k'(mx) - \psi_k'(x)\psi_k(mx)}{m\zeta_k(x)\psi_k'(mx) - \zeta_k'(x)\psi_k(mx)} \tag{2}$$

Using logarithmic derivatives of Riccati–Bessel functions, Eq. (2) can be written in a form more convenient for calculations [7]:

$$a_k = \gamma_k(x)\frac{\alpha_k(mx) - m\alpha_k(x)}{\alpha_k(mx) - m\beta_k(x)}$$
$$b_k = \gamma_k(x)\frac{m\alpha_k(mx) - \alpha_k(x)}{m\alpha_k(mx) - \beta_k(x)} \tag{3}$$

$$\alpha_k(z) = \psi_k'(z)/\psi_k(z) \quad \beta_k(z) = \zeta_k'(z)/\zeta_k(z)$$
$$\gamma_k(z) = \psi_k(z)/\zeta_k(z)$$

As was shown in Ref. [5], an alternative expression for the absorption efficiency factor may be obtained by integration of the internal (not external) electromagnetic field (see also Ref. [8]):

$$Q_a = \frac{2}{x^2}\sum_{k=1}^{\infty}\frac{2k+1}{|\zeta_k(x)|^2}\left\{\frac{\mathrm{Im}\big[m\alpha_k(mx)\big]}{|\beta_k(x) - m\alpha_k(mx)|^2} + \frac{\mathrm{Im}\big[m^*\alpha_k(mx)\big]}{|m\beta_k(x) - \alpha_k(mx)|^2}\right\} \tag{4}$$

where the asterisk (*) denotes a complex conjugate quantity. It can be shown that Eqs. (1) and (4) are mathematically equivalent [9].

The spectral emissivity of a particle may be determined from the solution of the fluctuation electrodynamics problem [10]. In this case, the final expression for ε_λ is identical to Eq. (4) [9,10]. This result confirms the Kirchhoff's law: $\varepsilon_\lambda \equiv Q_a$ [6,10].

It is well known that absorption of the radiation by a particle is, generally speaking, nonuniform over the volume of the particle. In the case of interaction of a plane electromagnetic wave with a homogeneous spherical particle, the amplitudes of the electric field components inside the particle are given by the following equations [5,6]:

$$E_r = \frac{E_0\cos\phi}{m^2\rho^2}\sum_{k=1}^{\infty} i^k(2k+1)d_k\psi_k(m\rho)P_k^{(1)}(\mu)$$

$$E_\theta = \frac{E_0\cos\phi}{m\rho}\sum_{k=1}^{\infty}\frac{i^k(2k+1)}{k(k+1)}\big[c_k\psi_k(m\rho)\pi_k(\mu) - id_k\psi_k'(m\rho)\tau_k(\mu)\big]$$

$$E_\phi = \frac{E_0\sin\phi}{m\rho}\sum_{k=1}^{\infty}\frac{i^{k+1}(2k+1)}{k(k+1)}\big[ic_k\psi_k(m\rho)\tau_k(\mu) + d_k\psi_k'(m\rho)\tau_k(\mu)\big] \tag{5}$$

where

$$c_k = \frac{mi}{m\zeta_k(x)\psi_k'(mx) - \zeta_k'(x)\psi_k(mx)}$$
$$d_k = \frac{mi}{\zeta_k(x)\psi_k'(mx) - m\zeta_k'(x)\psi_k(mx)}$$

$$\pi_k = \frac{P_k^{(1)}(\mu)}{\sqrt{1-\mu^2}} \qquad \tau_k(\mu) = -\sqrt{1-\mu^2}\frac{\mathrm{d}}{\mathrm{d}\mu}P_k^{(1)}(\mu)$$

Here, $\rho = 2\pi r/\lambda = (r/a)x$, $\mu = \cos\theta$, and the angle θ is measured from the direction of the incident wave, $P_k^{(1)}(\mu)$ is the associated Legendre polynomial. The value of the heat generation rate is equal to the power absorbed by a unit of volume of the particle [11–13]:

$$p_\lambda = \frac{4\pi n\kappa}{\lambda}I_\lambda^{(0)}\frac{\left(|E_r|^2 + |E_\theta|^2 + |E_\phi|^2\right)}{|E_0|^2} \tag{6}$$

where $I_\lambda^{(0)}$ is the spectral intensity of the incident radiation. After integration over the range of the angle θ, one can derive the following relation for the angle-averaged heat generation rate of a spherical layer of unit thickness (see also Ref. [12]):

$$P_\lambda(r) = \int_0^{2\pi}\int_0^{\pi}p_\lambda(r,\theta)\sin\theta\,\mathrm{d}\theta\,\mathrm{d}\phi = \frac{16\pi^2 n\kappa}{\lambda}I_\lambda^{(0)}S \tag{7}$$

$$S = \frac{1}{2|m|^4\rho^4}\sum_{k=1}^{\infty}(2k+1)\Big[k(k+1)|d_k\psi_k(m\rho)|^2 + |m|^2\rho^2\Big(|c_k\psi_k(m\rho)|^2 + |d_k\psi_k'(m\rho)|^2\Big)\Big]$$

The spectral emissivity of the particle may be expressed as follows:

$$\varepsilon_\lambda(x, m) = \frac{\int_0^a P_\lambda r^2 \, \mathrm{d}r}{\pi a^2 I_\lambda^{(0)}} = \frac{8n\kappa}{x^2} \int_0^x S\rho^2 \, \mathrm{d}\rho \tag{8}$$

Calculation by means of Eqs. (7) and (8) must give the same values of ε_λ as those calculated by Eq. (1) or (4) that are simpler: however, Eq. (7) also gives radial profiles of the heat source inside the particle. Eq. (8) may be used as a control of the accuracy of the heat source calculation.

3. The geometrical optics approximation

3.1. Numerical solution of the radiation transfer equation

The radiation transfer equation for a spherical volume of a nonscattering medium with an absorption coefficient $\Sigma_a(r)$ and a temperature profile $T(r)$ is as follows [14,15]:

$$\mu \frac{\partial I_\lambda}{\partial r} + \frac{1-\mu^2}{r} \frac{\partial I_\lambda}{\partial \mu} + \Sigma_a I_\lambda = 2\pi n^2 \Sigma_a B_\lambda(T) \tag{9}$$

Here, $I_\lambda(r, \mu)$ is the spectral radiation intensity at point r $(0 \le r \le a)$ in the direction $-1 \le \mu = \cos\theta \le 1$ (θ is measured from the direction of the r-axis) and is integrated over the azimuth. The boundary conditions (symmetry at $r = 0$ and Snell's law at $r = a$) are as follows:

$$I_\lambda(0, -\mu) = I_\lambda(0, \mu) \; I_\lambda(a, -\mu) = R(\mu) \, I_\lambda(a, \mu) \tag{10}$$

where $0 \le \mu \le 1$, $R(n, \mu)$ is the Fresnel's reflection coefficient for unpolarized radiation [16]:

$$R = \left(R_{\parallel} + R_{\perp}\right)/2 \tag{11}$$

$$R_{\parallel} = \left\{ \frac{\mu - n\sqrt{1 - n^2\left(1-\mu^2\right)}}{\mu + n\sqrt{1 - n^2\left(1-\mu^2\right)}} \right\}^2$$

$$R_{\perp} = \left\{ n\mu - \frac{\sqrt{1 - n^2\left(1-\mu^2\right)}}{n\mu + \sqrt{1 - n^2\left(1-\mu^2\right)}} \right\}^2 \quad \mu > \mu_c$$

$$R_{\parallel} = R_{\perp} = 1, \quad \mu \le \mu_c = \sqrt{1 - 1/n^2}.$$

The value of $R = 1$ for $\mu \le \mu_c$ corresponds to total internal reflection.

The angle-averaged heat generation rate for a spherical layer of unit thickness is equivalent to the divergence of the spectral radiation flux:

$$P_\lambda(r) = \frac{1}{r^2} \frac{\mathrm{d}}{\mathrm{d}r}\left(r^2 q_\lambda\right)$$
$$= \Sigma_a \left[4\pi n^2 B_\lambda(T) - \int_{-1}^{1} I_\lambda(r, \mu) \, \mathrm{d}\mu \right] \tag{12}$$

The spectral radiation intensity on the outer surface of the volume and the corresponding spectral radiation flux are defined as follows:

$$I_\lambda^{\mathrm{e}}(a, \mu_{\mathrm{e}}) = \left[1 - R(\mu)\right] I_\lambda(a, \mu),$$

$$\mu = \sqrt{1 - \left(1 - \mu_{\mathrm{e}}^2\right)/n^2}, \; 0 \le \mu_{\mathrm{e}} \le 1 \tag{13}$$

$$q_\lambda^{\mathrm{e}}(a) = \int_0^1 I_\lambda^{\mathrm{e}}(a, \mu_{\mathrm{e}}) \mu_{\mathrm{e}} \, \mathrm{d}\mu_{\mathrm{e}} = \int_{\mu_c}^1 \left[1 - R(\mu)\right] I_\lambda(a, \mu) \mu \, \mathrm{d}\mu$$

In the case of a homogeneous isothermal medium Σ_a, T = const), it is convenient to use dimensionless variables

$$\tau = \Sigma_a r \qquad \varphi(\tau, \mu) = I_\lambda / \left(2\pi n^2 B_\lambda\right) \tag{14}$$

and to introduce the following expressions:

$$\tau_0 = \Sigma_a a \qquad W_\lambda = P_\lambda / \left(2\pi \Sigma_a n^2 B_\lambda\right)$$
$$\varepsilon_\lambda = q_\lambda^{\mathrm{e}} / (\pi B_\lambda) \tag{15}$$

Note that the absorption coefficient and the optical thickness are related to the index of absorption and the diffraction parameter by the following simple expressions:

$$\Sigma_a = 4\pi\kappa/\lambda \qquad \tau = 2\kappa\rho \qquad \tau_0 = 2\kappa x \tag{16}$$

In the new variables, the radiation transfer equation (9), the boundary conditions (10), and Eqs. (12) and (13) can be written as follows:

$$\mu \frac{\partial \varphi}{\partial \tau} + \frac{1-\mu^2}{\tau} \frac{\partial \varphi}{\partial \mu} + \varphi = 1, \quad 0 \le \tau \le \tau_0, \; -1 \le \mu \le 1$$

$$\varphi(0, -\mu) = \varphi(0, \mu)$$

$$\varphi(\tau_0, -\mu) = R(\mu)\varphi(\tau_0, \mu), \quad 0 \le \mu \le 1$$

$$W_\lambda(\tau) = 2 - \int_{-1}^{1} \varphi(\tau, \mu) \, \mathrm{d}\mu$$
$$\varepsilon_\lambda = 2n^2 \int_{\mu_c}^{1} \left[1 - R(\mu)\right] \varphi(\tau_0, \mu) \mu \, \mathrm{d}\mu \tag{17}$$

Presenting the radiation intensity in the form

$$\varphi(\tau, \mu) = \begin{cases} \varphi^{-}(\tau, -\mu), & \mu < 0 \\ \varphi^{+}(\tau, \mu), & \mu > 0 \end{cases} \tag{18}$$

and introducing the functions [7]

$$g(\tau, \mu) = \varphi^{-} + \varphi^{+}$$
$$h(\tau, \mu) = \varphi^{-} - \varphi^{+}, \quad 0 < \mu \leq 1 \tag{19}$$

we obtain the following, instead of Eq. (17):

$$\mu \frac{\partial h}{\partial \tau} = g - \frac{1-\mu^2}{\tau} \frac{\partial h}{\partial \mu} - 2$$
$$\tau = 0, h = 0$$

$$\mu \frac{\partial g}{\partial \tau} = h - \frac{1-\mu^2}{\tau} \frac{\partial g}{\partial \mu}$$
$$\tau = \tau_0, \gamma g + h = 0$$

$$W_\lambda(\tau) = 2 - \int_0^1 g(\tau, \mu)\, \mathrm{d}\mu$$
$$\varepsilon_\lambda = n^2 \int_{\mu_c}^1 (1-R)\big[g(\tau_0, \mu) - h(\tau_0, \mu)\big]\mu\, \mathrm{d}\mu \tag{20}$$
$$= 2n^2 \int_{\mu_c}^1 \gamma g(\tau_0, \mu)\mu\, \mathrm{d}\mu$$

where $\gamma = (1-R)/(1+R)$. Replacing the variables (τ, μ) by (τ, y), where $y = \tau\sqrt{1-\mu^2}$, leads to much simpler combined equations:

$$\sqrt{1-(y/\tau)^2}\frac{\partial h}{\partial \tau} = g - 2 \qquad \sqrt{1-(y/\tau)^2}\frac{\partial g}{\partial \tau} = h \tag{21}$$

in the triangular computational region $0 \leq \tau \leq \tau_0$, $0 \leq y \leq \tau_0$. After transition to one second-order equation for the function $g(\tau, y)$, we have

$$\tau\big(\tau^2 - y^2\big)\frac{\partial^2 g}{\partial \tau^2} + y^2 \frac{\partial g}{\partial \tau} - \tau^3(g-2) = 0$$

$$\tau = 0, \quad \frac{\partial g}{\partial \tau} = 0$$
$$\tau = \tau_0, \quad \gamma g + \sqrt{1-(y/\tau)^2}\frac{\partial g}{\partial \tau} = 0 \tag{22}$$

where $\gamma = \gamma\big(n, \sqrt{1-(y/\tau)^2}\big)$. The parabolic problem (22) does not contain derivative $\partial g/\partial y$ and may be considered to be a set of separate boundary-value problems at different fixed values of y. After solving the problem (22), one can find $W_\lambda(\tau)$ and ε_λ by integration:

$$W_\lambda(\tau) = 2 - \frac{1}{\tau}\int_0^\tau \frac{g(\tau, y) y\, \mathrm{d}y}{\sqrt{\tau^2 - y^2}}$$
$$\varepsilon_\lambda = 2\frac{n^2}{\tau_0^2}\int_0^{\tau_0/n} \gamma g(\tau_0, y) y\, \mathrm{d}y \tag{23}$$

To calculate the value of ε_λ we can also use the following simple relation derived from the energy balance on the surface $\tau = \tau_0$:

$$\varepsilon_\lambda = \frac{2n^2}{\tau_0^2}\int_0^{\tau_0} W_\lambda(\tau)\tau^2\, \mathrm{d}\tau \tag{24}$$

The algorithm proposed remains unchanged in the case of a nonisothermal volume. It is sufficient to calculate the Planck's function in Eqs. (14) and (15), for instance, at the average temperature

$$\bar{T} = \frac{3}{a^3}\int_0^a T(r) r^2\, \mathrm{d}r \tag{25}$$

and to multiply the numerical coefficient 2 in Eqs. (22) and (23) for $W_\lambda(\tau)$ by the ratio $B_\lambda(T)/B_\lambda(\bar{T})$. Note that the emissivity has no sense in the case of nonisothermal volume and the radiative flux should be calculated immediately.

4. Comparison of calculations that use different theoretical models

4.1. The spectral emissivity of an isothermal particle

The main radiative properties of isothermal spherical particles were comprehensively analyzed in [7]. It was shown that, in the case of a semitransparent material with $\kappa \leq 0.01$, the spectral emissivity of the particle is weakly affected by changes in the refractive index over the interval $1 \leq n \leq 2$ with an arbitrary diffraction parameter outside of the Rayleigh scattering region. The following approximation is applicable in the range $1.5 \leq n \leq 2$, $0.002 \leq \kappa \leq 0.02$ [17]:

$$\varepsilon_\lambda = \frac{4n}{(n+1)^2}\big[1 - \exp(-5\kappa x)\big]$$
$$+ 5\kappa x (n-1)^2 \exp\big[-x(n-1)/5\big] \tag{26}$$

Eq. (26), taken together with an approximation for the transport scattering efficiency factor makes it possible to simplify radiation transfer calculations in disperse systems [7].

In this paper, we will concern ourselves with a comparison of the Mie solution and the radiation transfer calculations inside the particle. Some typical results in the range of optical thicknesses of most interest are presented in Fig. 1. One can see that the numerical sol-

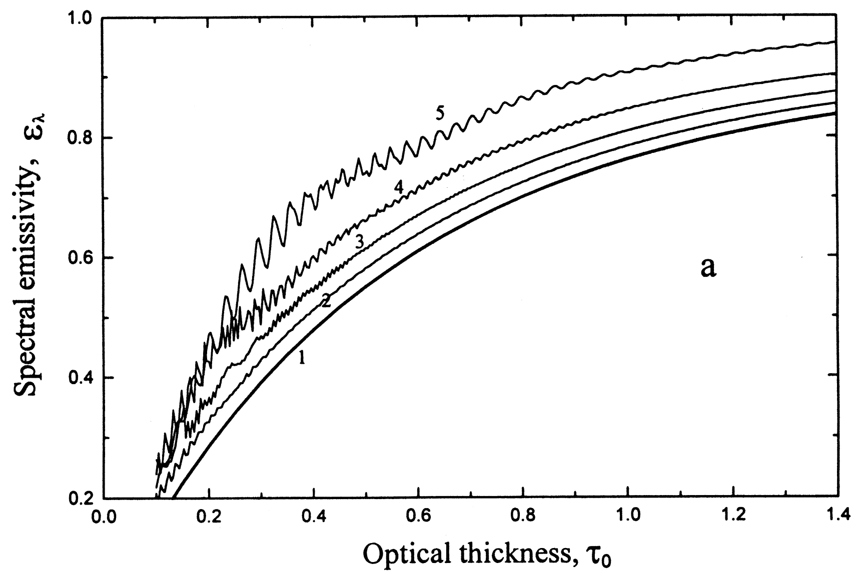

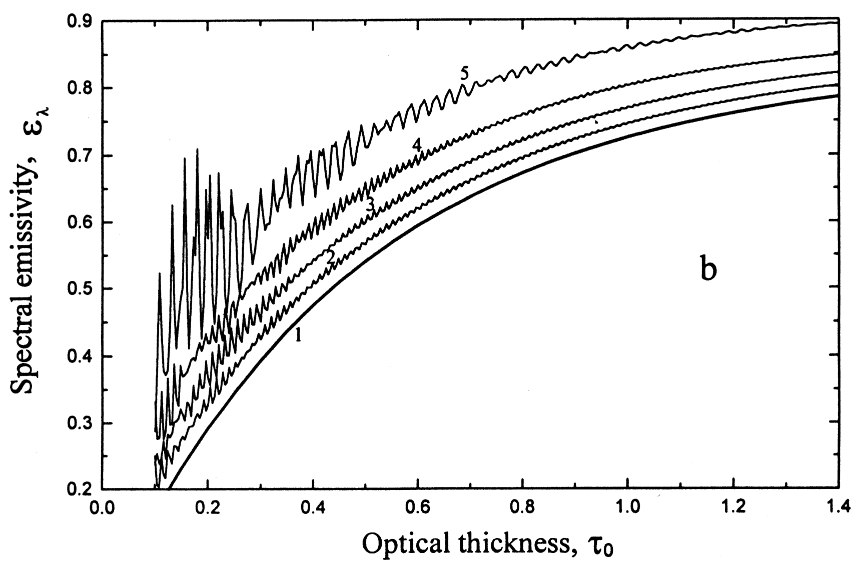

Fig. 1. Spectral emissivity of spherical particle at $n = 1.5$ (a) and $n = 2$ (b): 1 — numerical solution of the radiation transfer equation inside the particle, 2–5 — Mie theory calculations (2 — $\kappa = 0.002$, 3 — 0.005, 4 — 0.01, 5 — 0.02).

ution of the radiation transfer equation only slightly underestimates the emissivity of the particle when $\kappa < 0.01$ and $\tau_0 > 0.2$; it does not essentially differ from the asymptotic solution in the limit when $\kappa \to 0$.

Exact calculations of particle emissivity using the geometrical optics approximation are very simple in the case of $n = 1$, when the analytical solution is known. Note that it is more convenient to consider absorption of the incident plane wave by a particle instead of thermal radiation from a particle. The following expression for particle emissivity was derived by Van de Hulst [5] for optically soft particles

($x \gg 1$, $|m-1| \ll 1$):

$$\varepsilon_\lambda = 2\int_0^1 \left[1-\exp(-2\tau_0\mu)\right]\mu \, \mathrm{d}\mu = 1 + \frac{\exp(-2\tau_0)}{\tau_0} - \frac{1-\exp(-2\tau_0)}{2\tau_0^2} \qquad (27)$$

It is possible to compare numerical calculations using the algorithm proposed in Section 3 with the exact analytical solution (27). Because the angular dependencies of the radiation intensity are smooth, we can also employ the diffusion approximation and the corresponding analytical solution [5]:

$$\varepsilon_\lambda = \frac{4\sqrt{D}}{\left(4-\sqrt{4-N_\mathrm{a}N_\mathrm{m}}\right)\sqrt{D} + 1/\left[\coth\left(\tau_0/\sqrt{D}\right) - \sqrt{D}/\tau_0\right]} \qquad (28)$$

Here, $D = 1/(4-N_\mathrm{a})$ is the dimensionless radiation diffusion coefficient: N_a is equal to 0 for the DP_0-approximation and to 1 for the P_1-approximation; $N_\mathrm{m} = 0$ for the Marshak boundary condition and $N_\mathrm{m} = 1$ for the Pomraning one (the $P_{1\mathrm{m}}$-approximation) [7]. A comparison of different calculations is presented in Table 1. Note there is practically no difference between calculations using the Mie theory and those using the geometrical optics approximation for small values of the absorption index. We can also see that the error in the diffusion approximation is very small for an arbitrary optical thickness of the particle. It is interesting that all the theoretical models considered give the same result of $\varepsilon_\lambda = 4\tau_0/3$ in the limit when $\kappa, \tau_0 \ll 1$ for uniform heat generation over the volume of the particle.

In Ref. [18], the following more general expression for $Q_\mathrm{a} \equiv \varepsilon_\lambda$ obtained with the geometrical optics approximation when $\kappa \ll n$ was given (this expression was also derived in Ref. [19]):

$$\varepsilon_\lambda = \int_0^1 \left\{ \frac{1-R_{||}}{1-R_{||}\exp(-\tau_0 l)} + \frac{1-R_\perp}{1-R_\perp\exp(-\tau_0 l)} \right\} \times \left[1-\exp(-\tau_0 l)\right]\mu \, \mathrm{d}\mu \qquad (29)$$

Here, $l(\mu) = 2\sqrt{1-(1-\mu^2)/n^2}$ and $R_{||}(\mu), R_\perp(\mu)$ are defined in Eq. (11). For the optically thin limit ($\tau_0 \ll 1$), we find the following expression in Ref. [18]:

$$\varepsilon_\lambda = \frac{4\tau_0}{3} n^2 \left[1 - \left(1-1/n^2\right)^{3/2}\right] \qquad (30)$$

which was also derived in Refs. [6,20]. A more accurate equation that was derived when taking into account end effects may be found in Ref. [21].

To evaluate the error of the numerical solution of the radiation transfer equation, a comparison may be made with the tabulated data in Ref. [18], which were obtained by accurate integration of Eq. (29) (see Table 2). It is important that the computational error be much less than the difference between the geometrical optics approximation and the Mie theory solution (Fig. 1).

4.2. Heat generation distribution inside the particle

In the case of $n > 1$, internal heat generation is not uniform even for optically thin particles ($\tau_0 \ll 1$) (except for the Rayleigh region when $nx \ll 1$); it depends essentially on the diffraction parameter. This contention is illustrated in Fig. 2, where calculations using Eqs. (7) and (8) are presented in the form of dimensionless profiles:

$$\bar{W}_\lambda(\bar{r}) = \frac{W_\lambda(\bar{r})}{3\int_0^1 W_\lambda(\bar{r})\bar{r}^2 \, \mathrm{d}\bar{r}} = \frac{8}{3} n\kappa S(\bar{r})/\varepsilon_\lambda, \quad \bar{r} = r/a \qquad (31)$$

The effect of the absorption index, when $\kappa \leq 0.02$, is insignificant, whereas an increase of the refractive index, especially when $n > 1.5$, results in considerable deformation of the curves $W_\lambda(\bar{r})$. This deformation strongly depends on the value of the diffraction par-

Table 1
Spectral emissivity of non-refracting particles ($n = 1$)

	Mie theory		Radiation transfer theory		Diffusion approximation (28)		
τ_0	$\kappa = 0.01$	$\kappa = 0.001$	Numerical solution	Exact analytical solution (27)	DP_0	P_1	$P_{1\mathrm{m}}$
0.2	0.2317	0.2306	0.226	0.2306	0.2331	0.2336	0.2300
0.5	0.4729	0.4716	0.464	0.4715	0.4768	0.4823	0.4672
1	0.7047	0.7030	0.695	0.7030	0.6990	0.7201	0.6870
2	0.8884	0.8865	0.881	0.8864	0.8576	0.9033	0.8518
5	0.9821	0.9801	0.978	0.9800	0.9473	1.0106	0.9465

Table 2
Spectral emissivity of particles with index of refraction $n > 1$. Calculations in geometrical optics approximation

	Exact solution (29)		Numerical solution of radiation transfer equation		MDP_0-approximation	
τ_0	$n = 1.5$	$n = 2$	$n = 1.5$	$n = 2$	$n = 1.5$	$n = 2$
0.1	0.1582	0.1639	0.156	0.162	0.160	0.169
0.2	0.2889	0.2917	0.283	0.289	0.293	0.304
0.4	0.4790	0.4744	0.474	0.472	0.494	0.498
0.6	0.6100	0.5934	0.604	0.591	0.632	0.625
1	0.7626	0.7256	0.758	0.723	0.793	0.766
2	0.8831	0.8221	0.881	0.821	0.924	0.868
4	0.9074	0.8930	0.907	0.838	0.956	0.887
6	0.9082	0.8394	0.907	0.838	0.958	0.888

ameter. As usually in the case, the most complex interference effects are observed in the resonance range $2x(n-1) < 10$ [7]. For larger particles, we can expect a satisfactory description of the dependencies $W_\lambda(\bar{r})$ by radiation transfer theory. A comparison of the numerical solution of the problem (22) and the Mie theory calculations presented in Fig. 3 shows that, for sufficiently large particles ($x \geq 20$), the heat generation profile can be calculated without taking into account any interference effects for an arbitrary optical thickness of the particle. One can see that radiation transfer theory describes with sufficient accuracy the following special features of the internal radiation field: a displacement of the maximum of local heat generation from the center to the surface as the optical thickness of the particle increases; a change in the radial dependence of heat generation at the point $\bar{r} = 1/n$; and a relative increase in the thermal radiation emitted from the central region $\bar{r} < 1/n$ with increasing the index of refraction. The latter features of the heat generation distribution inside weakly absorbing particles were found previously in [12]. The discontinuity at $\bar{r} = 1/n$ was also found in [2] for dielectric spheres of $n = 1.33$, $x \geq 300$. The kink in the curves $W_\lambda(\bar{r})$ is explained by the internal reflection of radiation emitted by elementary volumes placed at $\bar{r} > 1/n$. One can find the position of the kink from a simple geometrical consideration.

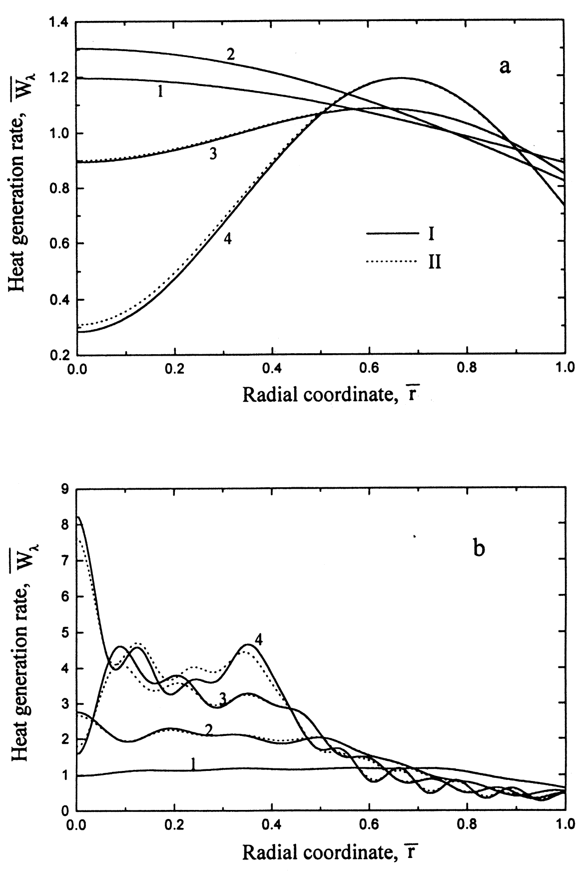

Fig. 2. Heat generation profiles in particles of moderate size. Mie theory calculations for $x = 1$ (a) and $x = 10$ (b): I — $\kappa = 0.01$, II — 0.02; 1 — $n = 1.5$, 2 — 2, 3 — 2.5, 4 — 3.

In spite of the comparatively simple physical model of radiation transfer, the calculated radiation field in a large refracting particle is rather complex, mainly, due to the effect of the total internal reflection at $\mu \leq \mu_c$. Some typical angular dependencies of the dimensionless radiation intensity are presented in Fig. 4, which illustrates the evolution of $\varphi(\bar{r}, \theta)$ as $\bar{r}$ varies from $1/n$ to 1 and due to refraction on the particle surface. The complex shape of the angular curves when $\bar{r} > 1/n$ indicates that the ordinary diffusion approximation is inapplicable for describing radiation transfer in the problem under consideration.

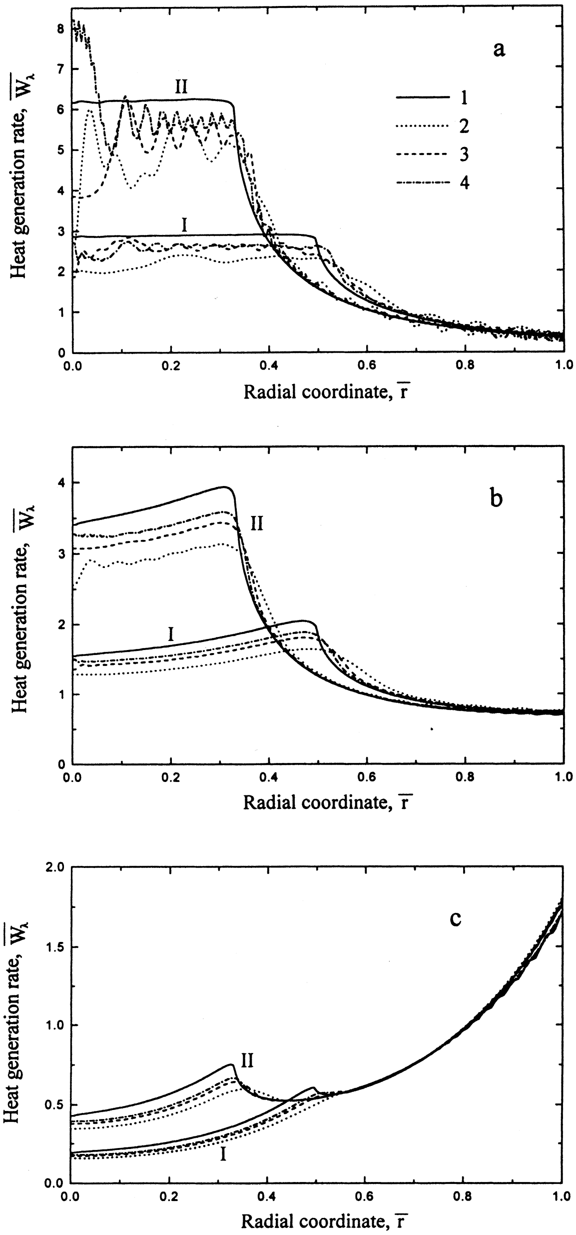

Fig. 3. Heat generation profiles in large particles at $\tau_0 = 0.2$ (a), 2 (b), and 5 (c): I — n = 2, II — 3; 1 — numerical solution of the radiation transfer equation, 2–4 — Mie theory calculations (2 — x = 20, 3 — 50, 4 — 100).

5. The modified differential approximation

An analysis of angular dependencies of the radiation intensity in the range $\tau_0/n < \tau \leq \tau_0$ (see Fig. 4) shows that the following approximation of the function $\varphi(\tau, \mu)$ may be rather good:

$$\varphi(\tau, \mu) = \begin{cases} \varphi_0^-(\tau), \ -1 \leq \mu < -\mu_* \\ 1, \ -\mu_* < \mu < \mu_* \\ \varphi_0^+(\tau), \mu_* < \mu \leq 1 \end{cases} \tag{32}$$

$$\mu_*(\tau) = \sqrt{1 - \left(\frac{\tau_0}{n\tau}\right)^2}$$

Integrating radiation transfer Eq. (17) over μ separately on intervals $-1 \leq \mu < \mu_*$ and $\mu_* < \mu \leq 1$, and introducing the functions

$$g_0 = \varphi_0^- + \varphi_0^+ \qquad h_0 = \varphi_0^- - \varphi_0^+ \tag{33}$$

we obtain after transformations the following coupled equations and the boundary condition:

$$-\frac{1 + \mu_*}{2} h_0' + g_0 = 2 \qquad -\frac{1 + \mu_*}{2} g_0' + h_0 = 0$$

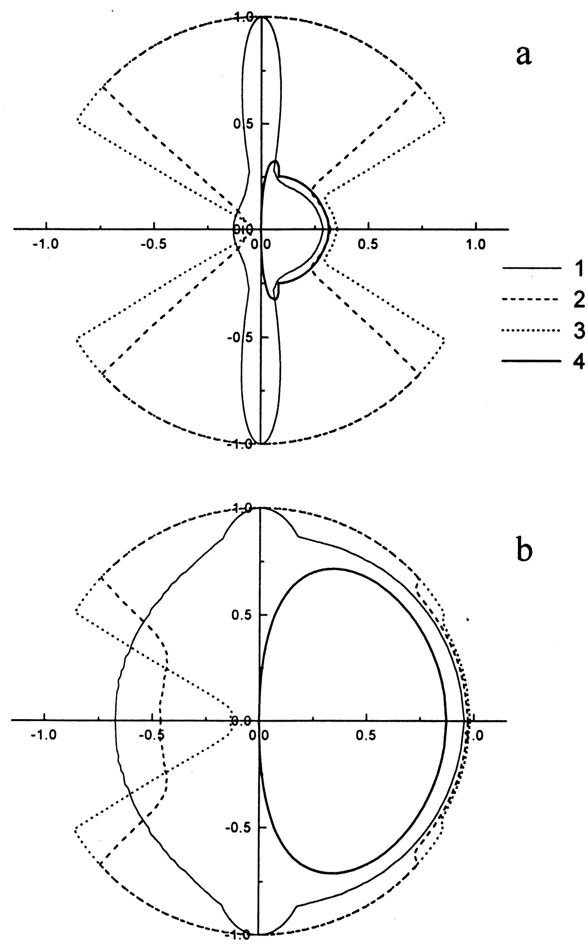

Fig. 4. Angular dependencies of dimensionless radiation intensity at n = 2 for particles with $\tau_0 = 0.2$ (a) and $\tau_0 = 2$ (b): 1 — $\bar{r} = 0.5$, 2 — $\bar{r} = 0.75$, 3 — $\bar{r} = 1 - \delta$, 4 — $\bar{r} = 1 + \delta (0 < \delta \ll 1)$.

$$\gamma^{(1)} g_0(\tau_0) + h_0(\tau_0) = 0$$
$$\gamma^{(1)} = (1 - R_1)/(1 + R_1) \tag{34}$$

For simplicity, the coefficient R_1 may be taken to be $R(1)$. In the central region $\tau \le \tau_0/n$, according to the usual DP_0-approximation [7], we have:

$$-\frac{1}{2}h_0' + \frac{h_0}{\tau} + g_0 = 2 \qquad -\frac{1}{2}g_0' + h_0 = 0 \tag{35}$$

and the symmetry condition $h_0(0) = 0$. Finally, the boundary-value problem in the modified DP_0-approximation (MDP_0) for an unknown function $g_0(\tau)$ can be written as follows:

$$-g_0''/4 - C_1 g_0'/(2\tau) + C_2(g_0 - 2) = 0 \tag{36}$$

$$C_1 = \begin{cases} 1, \tau \le \tau_0/n \\ (1-\mu_*)/(2\mu_*), \tau > \tau_0/n \end{cases}$$

$$C_2 = \begin{cases} 1, \tau \le \tau_0/n \\ (1+\mu_*)^{-2}, \tau > \tau_0/n \end{cases}$$

$$g_0'(0) = 0 \quad \gamma^{(1)} g_0(\tau_0) + \frac{1+\mu_c}{2} g_0'(\tau_0) = 0$$
$$\gamma^{(1)} = 2n/(n^2+1)$$

$$\bar{W}_\lambda(\tau) = (1-\mu_*)[2 - g_0(\tau)] \quad \varepsilon_\lambda = \gamma^{(1)} g_0(\tau_0)$$

The MDP_0-approximation is much simpler than the transfer equation. It is sufficient to note that the computational time on the same finite-difference mesh decreases in two orders of magnitude when the MDP_0 is used. At the same time, the error in MDP_0 is not large (see Table 2 and Fig. 5). It is important that the heat generation profiles calculated in MDP_0 may be considered to be a sufficiently accurate approximation of the exact Mie solution for large particles. Note that the MDP_0-approximation gives a correct value for ε_λ and a correct profile $\bar{W}_\lambda(\tau)$, even in the case of an optically thin particle.

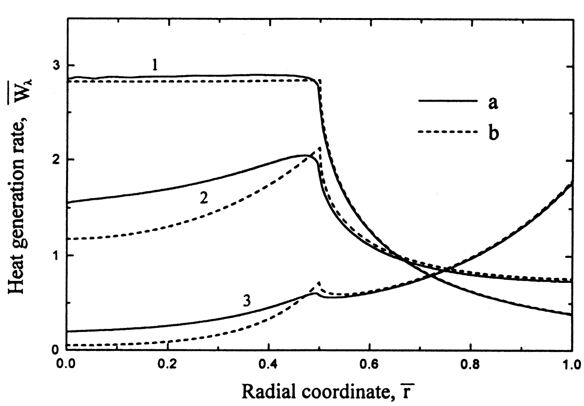

Fig. 5. Heat generation profiles calculated by numerical solution of the radiation transfer equation (a) and by use of MDP_0-approximation (b) at $n = 2$: 1 — $\tau_0 = 0.2$, 2 — 2, 3 — 5.

It is clear that calculations using MDP_0 are much faster than Mie calculations. For example, when $x = 100$, it takes about 14 s (on a Pentium-II, 266 MHz computer) to calculate the 500-point profile of the heat generation rate in a particle having diffraction parameter of $x = 100$ by Mie theory, whereas the time for the same calculation by MDP_0 is about 0.06 s.

6. Thermal radiation from a nonisothermal particle

To calculate the temperature profile in a large hot particle, which is cooled due to radiative and convective heat transfer with an ambient medium, we have to solve the transient radiative–conductive problem inside the particle with convective heat transfer in the boundary condition. Limited space does not allow us to consider this problem. We will present only several results for the parabolic temperature profile in the particle that qualitatively evaluates the nonuniform volumetric thermal radiation of the particle:

$$T(r) = T_0 - \frac{q_{\text{conv}}}{2ka} r^2 \tag{37}$$

Specifically, we set $T_0 = 3000$ K, $q_{\text{conv}}/k = 10$ K/μm. In this alternative, the surface temperature varies from $T_s = 2900$ to 2500 K when the radius of the particle increases from $a = 20$ to 100 μm. The integral radiative flux from the particle is defined as

$$q = \int_0^\infty q_\lambda \, d\lambda \tag{38}$$

Below, we consider the following relative quantities:

$$\bar{q} = q[T(r)]/q(T_s) \qquad \bar{q}_{\text{av}} = q(\bar{T})/q(T_s) \tag{39}$$

The results of calculations using the MDP_0-approximation for particles with a constant index of refraction $n = 2$ are presented in Fig. 6. We see that the contribution of the central hot region to the total thermal radiation from the particle decreases as the index of absorption increases. Nevertheless, the radiation from a particle of radius 20 μm remains greater than that calculated using the average temperature. For larger particles, there is a transition from conditions with radiation mainly from the central region radiation ($\bar{q} > \bar{q}_{\text{av}}$) to dominant radiation from the surface layer ($\bar{q} < \bar{q}_{\text{av}}$). This transition takes place at an optical thickness of the particle of $\tau_0 \approx 3.5$ (see Fig. 6), which

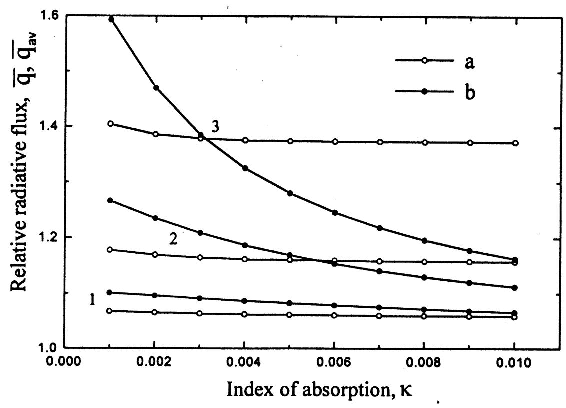

Fig. 6. Effect of the temperature profile on the particle thermal radiation: a — calculation by use of average temperature ($\bar{q}_{av}$), b — complete calculation ($\bar{q}$); 1 — a = 20, 2 — 50, 3 — 100 μm.

agrees well with evolution of the power profile of radiation shown in Fig. 5.

7. Conclusions

- The radial distribution of the heat source of thermal radiation in an isothermal spherical particle is analyzed using the Mie theory. Calculations showed that this distribution depends essentially on optical constants n, κ and also on the diffraction parameter x. For particles of a weakly absorbing material, the general solution degenerates at low and also at high values of the diffraction parameter. In both limits, the solution does not depend on the index of absorption κ, and we have only two parameters: n, x when $x \ll 1$ or n, $\tau_0 = 2\kappa x$ when $x \gg 1$. The latter limit corresponds to the region of the geometrical optics, where the radiation transfer theory may be applicable.
- A numerical solution of the radiation transfer equation inside a homogeneous spherical particle with Fresnel's boundary condition is obtained. A comparison with the Mie theory calculations for isothermal particles shows that the geometrical optics approximation is sufficiently accurate, even for particles that are not very large ($x \geq 20$), both for the particle emissivity value and for the heat generation profile. For typical indices of refraction, it is found that a transition from dominant thermal radiation of the central region to that of the surface layer takes place when the optical thickness of the particle is $\tau_0 \approx 3$–4.
- On the basis of the proposed approximate description of the angular dependence of the radiation intensity, coupled equations of the modified differential approximation (MDP_0) are derived. The MDP_0-approximation gives a sufficiently accurate solution for the thermal radiation field inside the particle, and the computational time is two orders of magnitude less than that of the numerical solution of the radiation transfer equation. This latter circumstance is very important for a numerical analysis of combined heat transfer problems in disperse systems containing high-temperature nonisothermal particles.
- A calculation of thermal radiation from single nonisothermal particles using the MDP_0-approximation shows that, for typical metal oxide particles of radius 100 μm with radial variation of temperature from 3000 to 2500 K, the error of the radiative flux calculation in the isothermal approximation using the volume-averaged temperature is at a level of $\pm 20\%$. A more rigorous analysis of the transient thermal state of a radiating particle should be based on the solution to the radiative–conductive heat transfer problem with account taken of the temperature varying complex index of refraction and the dynamics of crystallization. In this case, a generalization of the radiation transfer model for at least two-layer spherical particles is needed.

References

[1] T.G. Theofanous, The study of steam explosions in nuclear systems, Nuclear Engineering and Design 155 (1995) 1–26.
[2] H.M. Lai, P.T. Leung, K.L. Poon, K. Young, Characterization of the internal energy density in Mie scattering, J. Opt. Soc. Am. A 8 (1991) 1553–1558.
[3] D.Q. Chowdhury, P.W. Barber, S.C. Hill, Energy-density distribution inside large nonabsorbing spheres by using Mie theory and geometric optics, Applied Optics 31 (1992) 3518–3523.
[4] N. Velesco, T. Kaiser, G. Schweiger, Computation of the internal field of a large spherical particle by use of the geometrical-optics approximation, Applied Optics 36 (1997) 8724–8728.
[5] H.C. Van de Hulst, Light Scattering by Small Particles, Wiley, New York, 1957 (Chapters 9 and 11).
[6] C.F. Bohren, D.R. Huffman, Absorption and Scattering of Light by Small Particles, Wiley, New York, 1983 (Chapters 4 and 7).
[7] L.A. Dombrovsky, Radiation Heat Transfer in Disperse Systems, Begell House, New York, 1996 (Chapters 1 and 2).
[8] A.P. Prishivalko, V.A. Babenko, V.N. Kuzmin,

Scattering and Absorption of Light by Nonhomogeneous and Anisotropic Particles (in Russian), Nauka, Minsk, 1984 (Chapter 2).

[9] G.W. Kattawar, M. Eisner, Radiation from a homogeneous isothermal sphere, Applied Optics 9 (1970) 2685–2690.

[10] M.L. Levin, S.M. Rytov, Theory of Equilibrium Thermal Fluctuations in Electrodynamics (in Russian), Nauka, Moscow, 1967 (Chapter 2).

[11] A.P. Prishivalko, Optical and Thermal Fields in Light Scattering Particles (in Russian), Nauka, Minsk, 1983 (Chapter 1).

[12] D.W. Mackowski, R.A. Altenkirch, M.P. Mengüç, Internal absorption cross sections in a stratified sphere, Applied Optics 29 (1990) 1551–1559.

[13] A. Tuntomo, C.L. Tien, S.H. Park, Internal distribution of radiant absorption in a spherical particle, Journal of Heat Transfer 113 (1991) 407–412.

[14] M.N. Özisik, Radiative Transfer and Interactions with Conduction and Convection, Wiley, New York, 1973 (Chapter 8).

[15] R. Siegel, J.R. Howell, Thermal Radiation Heat Transfer, Hemisphere, New York, 1981 (Chapter 21).

[16] M. Born, E. Wolf, Principles of Optics, 4th ed., Pergamon Press, New York, 1968 (Chapter 1).

[17] L.A. Dombrovsky, Approximate expressions for calculation of main radiative properties of spherical particles in the Mie scattering region, Teplofizika Vysokikh Temperatur (in Russian) 28 (1990) 1242–1245.

[18] V.P. Pinchuk, N.P. Romanov, Absorption cross section for spherical particles of arbitrary size with moderate absorptance, Zhurnal Prikladnoj Spektroskopii (in Russian) 27 (1977) 109–116.

[19] G.M. Harpole, Radiative absorption by evaporating droplets, International Journal of Heat and Mass Transfer 23 (1980) 17–26.

[20] S. Twomey, C.F. Bohren, Simple approximations for calculations of absorption in clouds, Journal of Atmospheric Science 37 (1980) 2086–2094.

[21] A.A. Kokhanovskii, Influence of end effects on the light absorption by weakly absorbing spheres, Optics and Spectroscopy 78 (1995) 967–969.